International Journal of Precision Engineering and Manufacturing Vol. 5, No. 1, January 2004.

Trajectory Generation of a Moving Object for a Mobile Robot in Predictable Environment

TaeSeok Jin[1] and JangMyung Lee[2, #]

[1, 2] Department of Electronics Engineering, Pusan National University, Busan, South Korea

ABSTRACT

In the field of machine vision using a single camera mounted on a mobile robot, although the detection and tracking of moving objects from a moving observer, is complex and computationally demanding task. In this paper, we propose a new scheme for a mobile robot to track and capture a moving object using images of a camera. The system consists of the following modules: data acquisition, feature extraction and visual tracking, and trajectory generation. And a single camera is used as visual sensors to capture image sequences of a moving object. The moving object is assumed to be a point-object and projected onto an image plane to form a geometrical constraint equation that provides position data of the object based on the kinematics of the active camera. Uncertainties in the position estimation caused by the point-object assumption are compensated using the Kalman filter. To generate the shortest time trajectory to capture the moving object, the linear and angular velocities are estimated and utilized. The experimental results of tracking and capturing of the target object with the mobile robot are presented.

Key Words: Mobile robot, Kalman filter, Tracking & Capturing, Active camera, Trajectory generation

1. Introduction

Mobile robots have many application fields because of their high workability[1-6]. They are especially necessary for tasks that are difficult and dangerous for men to perform[22]. Many researchers have shown interest in mobile robots. Most of them have focused on successful navigation on reaching a fixed target point safely[7-8,10,12,18-21,24]. However, if a mobile robot is working under water or in space, the target object may move freely[11,14,22]. Therefore, the ability of a mobile robot to process moving targets is necessary. If an active camera system is applied to navigation and the tracking of moving objects, there will be many advantages[18,20]. An active camera system capable of panning and tilting should be able to automatically calibrate itself and keep track of an object of interest for a longer time interval without movement of the mobile robot[1]. There are several approaches[13, 15-17] that can be used to overcome the uncertainties of measuring the locations of the mobile robot or other objects.

In this paper, the position of an object was estimated using the kinematics of an active camera and images of the object assuming that it is flat and small on the floor. The linear and angular velocities of the object were estimated for the mobile robot to predict the future trajectory of the object, which plans the shortest time path to track and capture the moving object. A state estimator was designed to overcome the uncertainties from the image data caused by the point-object assumption and physical noises using a Kalman filter. Based on the estimated velocities of the object, the pose of the active camera was controlled to locate images of the object on the center of the image frame.

Manuscript received: February 24, 2003 ;
Accepted: November 17, 2003
Corresponding Author :
Email : jmlee@pusan.ac.kr
Tel. +82-51-510-1696 ; Fax +82-51-515-5190

2. Active Camera System

2.1 Kinematics of the active camera system

The active camera system has the ability of panning and tilting, as shown in Fig. 1. The position and posture of the camera are defined with respect to the base frame. According to the Denavit-Hartenberg convention, the homogeneous matrix Eq. (1) can be obtained after establishing the coordinate system and representing parameters, as shown in Fig. 1.

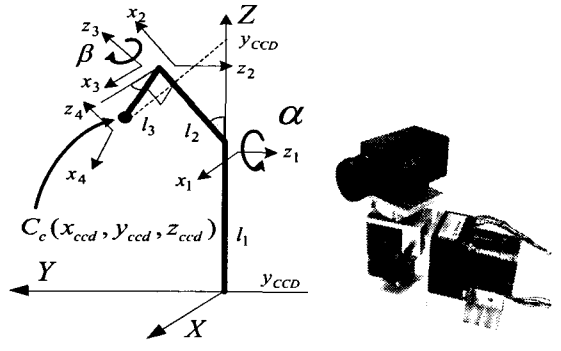

Fig. 1 Two d.o.f camera platform (Left) and its real image (Right).

$$
{}^0H_4 = {}^0H_1 \cdot {}^1H_2 \cdot {}^2H_3 \cdot {}^3H_4 =
\begin{bmatrix}
\cos(\alpha)\cos(\beta) & -\cos(\alpha)\sin(\beta) & \sin(\alpha) & l_2\sin(\alpha)+l_3\cos(\alpha)\cos(\beta) \\
\sin(\beta) & \cos(\beta) & 0 & l_3\sin(\beta) \\
-\sin(\alpha)\cos(\beta) & \sin(\alpha)\cos(\beta) & \cos(\alpha) & l_1+l_2\cos(\alpha)-l_3\sin(\alpha)\cos(\beta) \\
0 & 0 & 0 & 1
\end{bmatrix} \tag{1}
$$

In Fig. 1, Cc (x_{ccd}, y_{ccd}, z_{ccd}) represents a position vector from the center of the mobile robot to the center of camera lens. Each component of the vector can be represented in terms of tilting angle, α , and panning angle, β , of the CCD camera as follows:

$$x_{ccd} = l_2\sin(\alpha) + l_3\cos(\alpha)\cos(\beta) \tag{2}$$

$$y_{ccd} = l_3\sin(\beta) \tag{3}$$

$$z_{ccd} = l_1 + l_2\cos(\alpha) - l_3\sin(\alpha)\cos(\beta). \tag{4}$$

Also, an attitude vector of the homogeneous matrix represents Roll(θ_R), Pitch(θ_P) and Yaw(θ_Y) angles by tilting and panning angles of the camera as follows:

$$\theta_R = \tan^{-1}\left(\frac{\sin(\alpha)\sin(\beta)}{\sqrt{\cos^2(\alpha)\sin^2(\beta)+\cos^2(\beta)}}\right) \tag{5}$$

$$\theta_P = \tan^{-1}\left(\frac{\sin(\alpha)\cos(\beta)}{\sqrt{\cos^2(\alpha)\cos^2(\beta)+\sin^2(\beta)}}\right) \tag{6}$$

$$\theta_Y = \beta. \tag{7}$$

2.2 Relation between a camera and real coordinates

To measure the distance from a camera to an object using the camera images, at least two image frames that are captured for the same object at different locations, are necessary. Usually a stereo-camera system has been used to obtain the distance information [21]. However there exist uncertainties in feature point matching and it takes too much time to be implemented in real-time. The proposed approach requires only a frame to measure the distance to the object from the CCD camera [24]. Since it is possible by assuming that a point-object is located on the floor, there also exist uncertainties in the position estimation. To minimize the uncertainty in the position estimation and to estimate the velocities of the moving object together, a state estimator is designed based on the Kalman filter.

The image coordinates for the point object, (j , k), is transformed into the image center coordinates which is orientation invariant in terms of the Roll angle in Eq. (6), θ_R , and the size of the image frame, P_x and P_y , (j' , k'):

$$\begin{bmatrix} j' \\ k' \end{bmatrix} = \begin{bmatrix} \cos(\theta_R) & -\sin(\theta_R) \\ \sin(\theta_R) & \cos(\theta_R) \end{bmatrix} \begin{bmatrix} j - \frac{P_x}{2} \\ k - \frac{P_y}{2} \end{bmatrix} \tag{8}$$

where P_x and P_y represent x and y directional size of the image frame in pixels respectively.

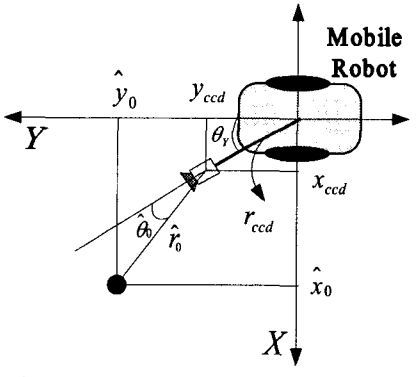

Fig. 2 Estimation of position information from a mobile robot.

To estimate the real location, (x_0 , y_0), $\hat{\theta}_0$ and $\hat{r}_0$ are estimated using the linear relationship between the real object range within the view angle and the image frame. That is, for a given set of ($\hat{\theta}_0$, $\hat{r}_0$), there is one-to-one correspondence between the real object point and the image point.

When a point image is captured at (j' , k') on the image center frame, the real object position, $\hat{\theta}_0$ and $\hat{r}_0$, can be estimated as follows, as illustrated in Fig. 3:

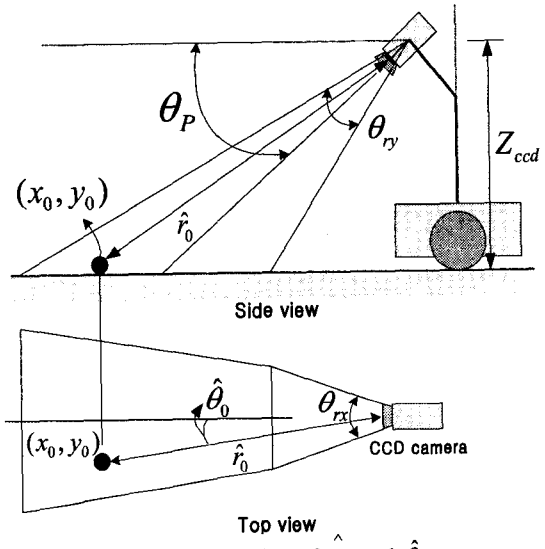

Fig. 3 Estimation of $\hat{r}_0$ and $\hat{\theta}_0$.

$$\hat{r}_0 = \frac{z_{ccd}}{\cot(\frac{\pi}{2} - \theta_P + \frac{k'}{P_y}\theta_{ry})} \tag{9}$$

$$\hat{\theta}_0 = \frac{j'}{P_x}\theta_{rx} \tag{10}$$

where θ_{rx} and θ_{ry} represent the x and y directional view angles of the CCD camera, respectively.

The position of the object with respect to the robot coordinates, (x, y) can be estimated using the $\hat{\theta}_0$ and $\hat{r}_0$ [8] as follows:

$$\hat{x}_0 = r_{ccd} \cdot \cos(\theta_Y) + \hat{r}_0 \cdot \cos(\theta_Y + \hat{\theta}_0) \tag{11}$$

$$\hat{y}_0 = r_{ccd} \cdot \sin(\theta_Y) + \hat{r}_0 \cdot \sin(\theta_Y + \hat{\theta}_0) \tag{12}$$

where θ_Y represents the angle between the robot and the active camera, and r_{ccd} (= $\sqrt{x^2_{ccd} + y^2_{ccd}}$) represents the distance from the robot to the center of the camera.

2.3. Inverse kinematics for placing the center of an image to the desired position

In the case of using an active camera, visual information on the area to be searched can be obtained through the inverse kinematics. The inverse kinematics equations that describe the attitude of the actuator used to place the center of an image onto a desired position, can be derived from Eq.'s (2)-(4) as follows:

$$\alpha_d = \cos^{-1}\left(\frac{-l_1 l_2 + \sqrt{l_1^2 l_2^2 - (l_1^2 + r_d^2)(l_1^2 - r_d^2)}}{(l_1^2 + r_d^2)}\right)\left(\frac{1}{\sin(\beta_d)}\right) \tag{13}$$

$$\beta_d = \tan^{-1}\left(\frac{y_d}{x_d}\right) \tag{14}$$

where α_d and β_d are the attitude of the camera, (x_d , y_d) represents the desired position of the camera, and r_d is $\sqrt{x_d^2 + y_d^2}$.

Table 1 shows parameters for the camera system, which are used in the Eq.'s (13) and (14)

Table 1 Parameters for the active camera system.

l_1	40 cm	l_2	7.5 cm
l_3	4 cm	-	-
P_x	320 pixel	P_y	240 pixel
θ_{rx}	50°	θ_{ry}	40°

3. Trajectory estimation of a moving object

3.1. Modeling of a moving object

When the velocity and acceleration of the target object can be estimated, the next target position $(\hat{T}_x, \hat{T}_y)$ can be predicted as follows [2]:

$$\hat{T}_{x+\delta t} = \hat{T}_x + \hat{V}_x \delta t + \frac{1}{2}\hat{A}_x \delta t^2 \tag{15}$$

$$\hat{T}_{y+\delta t} = \hat{T}_y + \hat{V}_y \delta t + \frac{1}{2}\hat{A}_y \delta t^2 \tag{16}$$

where δt is the sampling time, and $(\hat{T}_x, \hat{T}_y)$, $(\hat{V}_x, \hat{V}_y)$ and $(\hat{A}_x, \hat{A}_y)$ are the current Cartesian coordinate

estimates of the target position, velocity and acceleration respectively.

In the X-Y coordinates, movement of the object can be decomposed into the linear velocity element and the angular velocity element, as follows [3]:

$$\delta x_{k+\delta t,k} = v_k \delta t \cos(\theta_k + \frac{1}{2}\omega_k \delta t) \tag{17}$$

$$\delta y_{k+\delta t,k} = v_k \delta t \sin(\theta_k + \frac{1}{2}\omega_k \delta t) \tag{18}$$

$$\delta\theta_{k+\delta t,k} = \omega_k \delta t \tag{19}$$

$$\delta v_{k+\delta t,k} = \xi_v \tag{20}$$

$$\delta\omega_{k+\delta t,k} = \xi_\omega \tag{21}$$

where v_k and w_k are the variations of linear velocity and angular velocities w.r.t the target object moving on the x-y coordinates, and ξ_v and ξ_ω are the variations of linear velocity and angular velocity considering the moving object as random movement respectively.

From (17)-(21), we can obtain the state transition matrix, as follows:

$$\begin{aligned} \mathbf{x}_k &= \Phi_{k,k-1}\mathbf{x}_{k-1} + \mathbf{w}_{k-1} \\ \mathbf{Z}_k &= \mathbf{H}_k\mathbf{x}_k + \mathbf{v}_k \end{aligned} \tag{22}$$

where

$$\mathbf{x}_k = \begin{bmatrix} x_k \\ y_k \\ \theta_k \\ v_k \\ \omega_k \end{bmatrix}, \Phi_{k,k-1} = \begin{bmatrix} 1 & 0 & 0 & \delta t\cos(\theta_{k-1}) & -\frac{1}{2}v_{k-1}\delta t^2\sin(\theta_{k-1}) \\ 0 & 1 & 0 & \delta t\sin(\theta_{k-1}) & \frac{1}{2}v_{k-1}\delta t^2\cos(\theta_{k-1}) \\ 0 & 0 & 1 & 0 & \delta t \\ 0 & 0 & 0 & 1 & 0 \\ 0 & 0 & 0 & 0 & 1 \end{bmatrix},$$

$$\mathbf{Z}_k = \begin{bmatrix} x_k \\ y_k \end{bmatrix}, \mathbf{H}_k = \begin{bmatrix} 1 & 0 & 0 & 0 & 0 \\ 0 & 1 & 0 & 0 & 0 \end{bmatrix}, \mathbf{v}_k = \begin{bmatrix} \gamma_x \\ \gamma_y \end{bmatrix}, \text{ and}$$

$\mathbf{w}_{k-1} = [0\ 0\ 0\ \xi_v\ \xi_\omega]^T$.

Notice that Φ_k is the state transition matrix, $\mathbf{w}_k$ is the vector representing process noise, $\mathbf{Z}_k$ is the measurement vector, $\mathbf{H}_k$ represents the relationship between the measurement and the state vector, and γ_x and γ_y are x and y directional measurement errors respectively.

3.2. State estimation of a moving object based on a Kalman filter

Input data such as image information include uncertainties and noises generated during the data capturing and processing steps. And the state transition of a moving object also includes irregular components. Therefore as a robust state estimator against these irregularities, a Kalman filter was adopted to form a state observer [11-14]. The Kalman filter minimizes the estimation error by modifying the state transition model based on the error between the estimated vectors and the measured vectors with an appropriate filer gain. The state vector, which consists of position on the x-y plane, linear/angular velocities, and linear/angular accelerations can be estimated using the measured vectors representing the position of a moving object on the image plane.

The covariance matrix of estimated error must be calculated to determine the filter gain. The projected estimate of the covariance matrix of estimated error is represented as

$$P'_k = \Phi_{k,k-1}P_{k-1}\Phi^T_{k,k-1} + Q_{k-1} \tag{23}$$

where P'_k is a zero-mean covariance matrix representing the prediction error, Φ_k represents system noise, P_{k-1} is an error covariance matrix for the previous step, and Q_{k-1} represents other measurement and computational errors .

The optimal filter gain K_k that minimizes the errors associated with the updated estimate is

$$K_k = P'_k H^T_k [H_k P'_k H^T_k + R_k]^{-1} \tag{24}$$

where H_k is the observation matrix and R_k is the zero-mean covariance matrix of the measurement noise.

The estimate of the state vector $\hat{x}_k$ from the measurement Z_k is expressed as

$$\hat{x}_k = \Phi_{k,k-1}\hat{x}_{k-1} + K_k[Z_k - H_k\Phi_{k,k-1}\hat{x}_{k-1}]. \tag{25}$$

Therefore, $\hat{x}_k$ is updated based on the new values provided by Z_k . The error covariance matrix that will be used for the prediction, P_k , can be updated as follows [4,9];

$$P_k = P'_k - K_k H_k P'_k \tag{26}$$

After the current time is updated to $k+1$, a new estimation can be provided using Eqs. (23) to (26).

Fig. 4(a) represents a real and an estimated trajectories of a moving object, while Fig. 4(b) represents the estimation |error| when the trajectory was estimated by the Kalman filter.

To incorporate the measurement noise which is empirically assumed to be zero-mean, Gaussian random noise with the variance of 2, the linear and angular velocities of the object were set as follows:

$$\begin{aligned} v_k &= 15*(\sin(0.02*k)+1) + \xi_v \quad [\text{cm/sec}] \\ \omega_k &= 0.7*\cos(0.01*k) + \xi_\omega \quad [\text{rad/sec}] \end{aligned} \tag{27}$$

where the linear and angular velocities (ξ_v , ξ_w) were assumed to include the Gaussian random noise with the variance of 3 and 0.1, respectively.

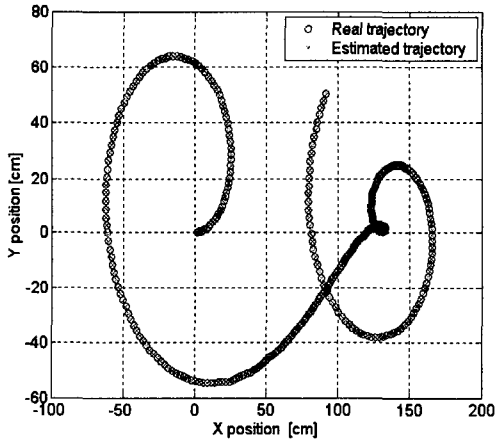

(a) Trajectory of moving object.

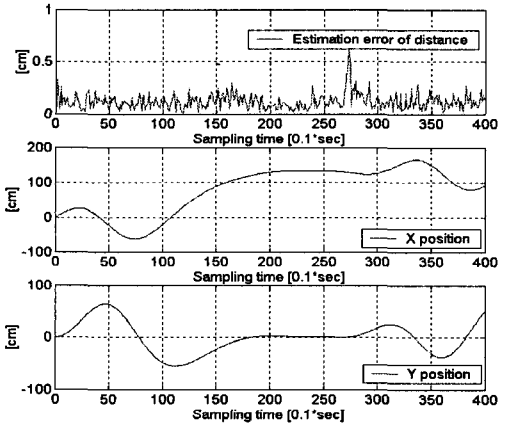

(b) Estimation error along the trajectory.

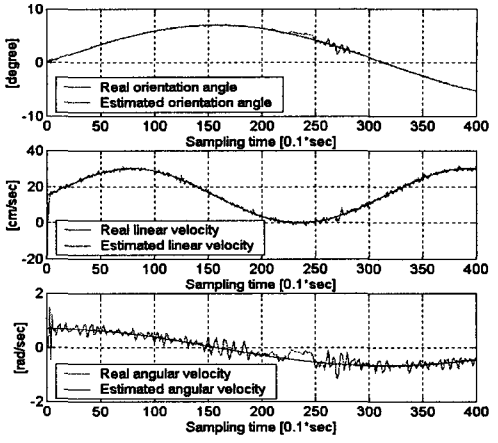

(c) State estimations, θ_k , v_k , and ω_k , using a Kalman filter.

Fig. 4 State estimations using a Kalman filter.

Fig. 4(a),(b) shows that the trajectory of a moving object, the estimation error and estimation of x, y coordinates of an object. And Fig. 4(c) shows the Kalman filter estimation of the states under a noisy environment.

3.3. Trajectory estimation of a moving object

The states of a moving object can be estimated if the initial state and input are given for the state transition model. Therefore, the states can be estimated for the next inputs by estimating the linear velocity and angular velocity of the moving object using the Kalman filter as a state estimator. From the linear velocity/acceleration and rotational angular velocity/acceleration data, the next states can be approximated as the following first order equations:

$$v_{k+n} = \hat{v}_k + \hat{a}_{lk} nT \tag{28}$$

$$\omega_{k+n} = \hat{\omega}_k + \hat{a}_{\omega k} nT \,. \tag{29}$$

In Fig. 4(c), the result includes possible noise since it is a dynamically varying system, although it is surpressed by the Kalman filter. Therefore the least square estimation method is utilized, which has robust anti-noise characteristics [23].

$$\hat{E} = (A^T A)^{-1} A^T y \tag{30}$$

where $\hat{E} = \begin{bmatrix} \hat{v}_k & \hat{\omega}_k \\ \hat{a}_{lk} & \hat{a}_{\omega k} \end{bmatrix}$, $A = \begin{bmatrix} 1 & -T \\ 1 & -2T \\ : & : \\ 1 & -mT \end{bmatrix}$, and

$y = \begin{bmatrix} v_{k-1} & \omega_{k-1} \\ v_{k-2} & \omega_{k-2} \\ : & : \\ v_{k-m} & \omega_{k-m} \end{bmatrix}$.

From the estimated inputs and using the state transition model, the trajectory of a moving object can be estimated as follows:

$$\hat{x}_{k+m} = x_k + \sum_{h=0}^{m} v(h)\cos[\theta(h)]T \tag{31a}$$

$$\hat{y}_{k+m} = y_k + \sum_{h=0}^{m} v(h)\sin[\theta(h)]T \tag{31b}$$

$$v(h) = \hat{v}_k + \hat{a}_{lk}hT \tag{32a}$$

$$\theta(h) = \hat{\theta}_k + \hat{\omega}_k hT + \frac{1}{2}\hat{a}_{\omega k}hT^2 . \tag{32b}$$

4. Motion planning for capturing

To capture a moving object, the mobile robot needs to be controlled by considering the relation between the position of the mobile robot and the position of the moving object. Fig. 5 shows the motion planning process of a mobile robot for capturing a moving object.

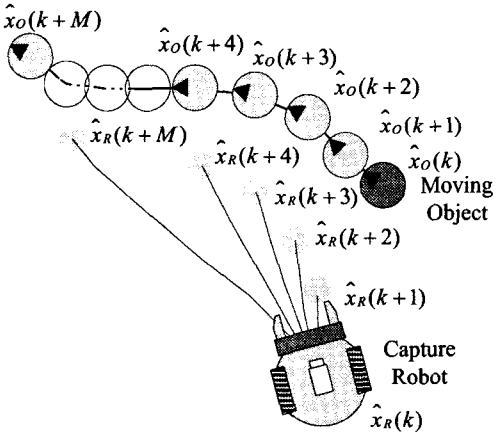

Fig. 5 Estimation of the trajectory for capturing.

The mobile robot estimates the position of the moving object within m sampling time and selects the shortest distance from its current position to the moving object, assuming that its location is known *a priori*. The localization scheme of the mobile robot using the information on the moving object, which improves the accuracy in capturing, is developed in [14]. The target point of the mobile robot at k-th sampling time is denoted as $\hat{x}_R(k+M)$, which is one of the estimated points of the mobile robot after m sampling time.

$$\hat{x}_R(k+M_{opt}) = \min_{m=1\sim M} \left\| \hat{x}_O(k+M) - \hat{x}_R(k+M) \right\| \tag{33}$$

where $\hat{x}_R(k+M)$ is the position of the mobile robot after m sampling time, and the mobile robot moves along the shortest path towards the target point $\hat{x}_O(k+M)$.

The position of the moving object in the cartesian coordinate system is acquired using the relation between image frames. The linear and angular velocities of the moving objects are estimated by the state estimator, Kalman filter.

After estimating the trajectory of the target object, the optimal trajectory and motion planning of the mobile robot are decided in order to capture the target object in the shortest time. The following figure shows the overall structure of mobile robot control for capturing a target object.

5. Simulations and Experiments

To demonstrate and illustrate the proposed method, we present an example. It is assumed that the velocity limit of a mobile robot is 30 cm/sec and the camera is installed on top of the mobile robot. The initial locations of the mobile robot and the moving object are (-50, -50) and (-250, 300) in cm with respect to the reference frame, respectively. The velocity and angular velocity of moving object are as follows:

$$v_k = 30(\cos(0.01k)+1) + \xi_v \quad [cm/\sec] \tag{34}$$

$$\omega_k = 0.7\sin(0.03k + \frac{\pi}{1.5}) + \xi_\omega \quad [rad/\sec] . \tag{35}$$

The forward direction and rotational angular velocity of the moving object are Gaussian random variable with variances of 2 and 0.1, respectively, which

are obtained experimentally.

Fig. 6(a) presents the trajectory of a moving object and the mobile robot trying to capture the object by estimating the trajectory. Fig. 6(b) represents the distance between the mobile robot and the moving object, the error between the estimated velocity and the real velocity, and the error between the estimated angular velocity and the real angular velocity respectively. Although the error of the estimated velocities is high at first, they converge to zero immediately.

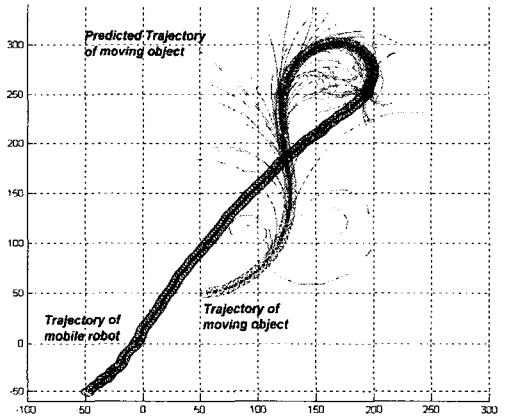

(a) Trajectory.

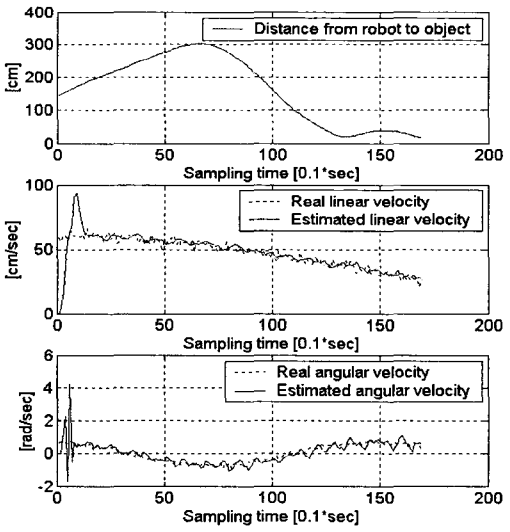

(b) Estimated state.

Fig. 6 Results of simulation.

Experiments that include the proposed algorithm are applied to a mobile robot named ZIRO developed in the laboratory [5], as shown in Fig. 7.

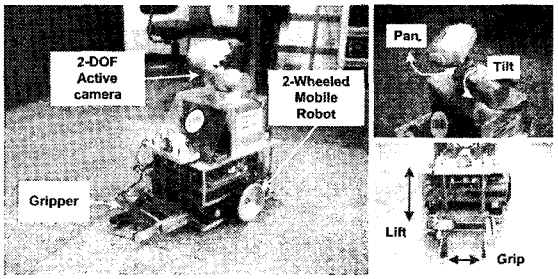

Fig. 7. Components of ZIRO.

ZIRO, the mobile robot used for this experiment, recognizes an object in the 3D space, approaches to the object to capture, and carries it to a goal position. For this purpose, ZIRO has a 2 d.o.f active camera to search and track an object and a gripper to capture the object. The two-wheel differential driving mechanism supports flexible motion on a floor following the commands based on the image captured by the 2 d.o.f pan/tilt camera.

To control the wheels in real time, a distributed control system is implemented using a CAN based network. Three CAN-based controllers are connected to the network, among which a controller gathers the gyro sensor data and sends them to the wheel controllers. The CAN network is connected to a higher-level ISA bus which connects the 2 d.o.f pan/tilt camera controllers to a main controller (a Pentium PC board). Every 100msec, the position of an object in 3D space is calculated using the posture of the camera and the object position on the image frame to plan the trajectory of the mobile robot. The planned trajectory commands was sent to the wheel controllers that uses PID algorithm to control the angle every 10 msec.

Experiment was performed to show the tracking and capturing a mobile object. Fig. 8 shows the experimental results for tracking and capturing a moving object that is an 8x6[cm] red-colored mouse and has two wheels with random velocities in the range of 25-35[cm/sec]. First, ZIRO detects the moving object using an active camera. When a moving object is detected within view, ZIRO tracks it following the proposed method. And Fig. 8 illustrates that the mobile robot captured a ball, moved to the target point and put the ball on the target point. The

minimum path was estimated using the trajectories of the mobile robot and the object, while the mobile was tracking the object. When the object is coming into the gripper, it grasps the object rigidly with the aid of the touch sensors.

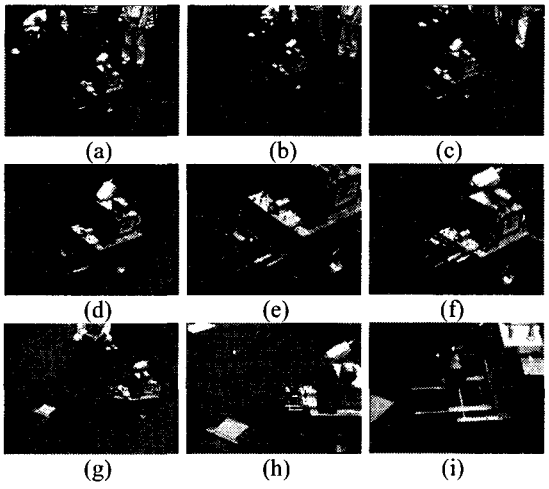

Fig. 8 Experiments for capturing a ball.

6. Conclusions

This paper proposes a method of tracking and capturing a moving object using an active camera mounted on a mobile robot. It describes a control scheme used for real-time tracking and capturing of objecting moving in front of the mobile robot. The new proposed scheme controls the system to maintain the position and distance to the moving object and to generate the shortest trajectory to the object.

The effectiveness of the proposed method is demonstrated by the simulation and experiments, and is verified through the following procedure:

1. Position estimation of a target object based on the kinematic relationship of consecutive image frames.
2. Movement estimation of the target object using a Kalman filter for tracking.
3. Motion planning of a mobile robot to capture the target object based on its estimated trajectory within the shortest time.

The approach enables real time tracking and capturing operations since it extracts the distance information from a single image frame and estimates the next motion using the Kalman filter which provides a closed form solution.

References

1. K. Daniilidis, C. Krauss, "Real-Time Tracking of Moving Objects with an Active Camera," Real-time imaging, Academic Press Limited, 1998.
2. Russell F. Berg, "Estimation and Prediction for Maneuvering Target Trajectories," IEEE Trans. on Automatic Control, Vol. AC-38, No.3, 1983.
3. Steven M. Lavalle and Rajeer Sharma, "On Motion Planning in Changing Partially Predictable Environments," The Int'l, Journal of Robotics Research, Vol. 16, No. 6, pp. 705-805, 1997.
4. H. W. Sorenson, "Kalman Filtering Techniques," Advances in Control Systems Theory and Applications, Vol. 3, pp.219-292, 1996.
5. Park, J. W., Lee, J. M., "Robust Map Building and Navigation for a Mobile Robot using Active Camera," Proc. of ICMT, pp.99-104, 1999.
6. R. A. Brooks, "A Robust Layered Control System for a Mobile Robot," IEEE Journal of Robotics and Automation, Vol. RA-2, No. 1, pp.14-23, 1986.
7. John J. Leonard and Hugh F. Durrant-Whyte, "Mobile Robot Localization by Tracking Geometric Beacons," IEEE Trans. Robotics and Automation, Vol. 7, No.3, pp. 376~382, 1991.
8. J. David, Kreigman et al., "Stereo vision and navigation in buildings for mobile robots," IEEE Trans. Robotics and Automation, Vol. 5, No. 6, pp. 792~803, 1989.
9. R. E. Kalman, "A New Approach to Linear Filtering and Prediction Problems," Trans, ASME, J. Basic Eng, Series 82D, pp. 35-45, 1960.
10. Han, M. Y., Kim, B. K., Kim, K. H. and Lee, Jang M. "Active Calibration of the Robot/Camera Pose Using the Circular Objects, Transactions on Control, Automation and Systems Engineering, Vol. 5, No. 3, pp. 314-323, 1999.
11. Dinesh Nair and Jagdishkumar K. Aggarwal, "Moving Obstacle Detection From a Navigation Robot," IEEE Trans. Robotics and Automation, Vol. 14, No. 3, pp. 404~416, 1989.
12. Anthony LALLET and Simon LACROIX, " Toward Real-Time 2D Localization in Outdoor Environ-

ments," Proceedings of the 1998 IEEE International Conference on Robotics & Automation, pp. 2827-2832, 1998.
13. A. Adam, E. Rivlin, and I. Shimshoni, "Computing the Sensory Uncertainty Field of a Vision-based Localization Sensor," Proceedings of the 2000 IEEE International Conference on Robotics & Automation, pp. 2993-2999, 2000.
14. Kim, B. H., Roh, D. K., Lee, J. M. Lee, M. H., Son, K. Lee, M. C., Choi, J. W. and Han, S. H. "Localization of a Mobile Robot using Images of a Moving Target," Proceedings of the 2001 IEEE International Conference on Robotics & Automation, 2001.
15. Vincenzo Caglioti, "An Entropic Criterion for Minimum Uncertainty Sensing in Recognition and Localization Part II-A Case Study on Directional Distance Measurements," IEEE Trans. On Systems, Man, and Cybernetics, Vol. 31, No. 2, pp. 197-214, 2001.
16. Clark F. Olson, "Probabilistic Self-Localization for Mobile Robots," IEEE Trans. On Robotics and Automation, Vol. 16, No. 1, pp. 55-66, 2000.
17. Hongjun Zhou and Shigeyuki Sakane, "Sensor Planning for Mobile Robot Localization Based on Probabilistic Inference Using Bayesian Network," Proceedings of the 4th IEEE International Symposium on Assembly and Task Planning, pp. 7-12, 2001.
18. Muriel Selsis, Christophe Vieren, and Francois Cabestaing, "Automatic Tracking and 3D Localization of Moving Objects by Active Contour Models," Proceedings of the 95 IEEE International Symposium on Intelligent Vehicles, pp. 96-100, 1995.
19. Howie Choset and Keiji Nagatani, "Topological Simultaneous Localization and Mapping (SLAM): Toward Exact Localization Without Explicit Localization," IEEE Trans. On Robotics and Automation, Vol. 17, No. 2, 2001.
20. Sanisa Segvic and Slobodan Ribaric, "Determining the Absolute Orientation in a Corridor Using Projective Geometry and Active Vision," IEEE Trans. On Industrial Electronics, Vol. 48, No. 3, pp. 696-710, 2001.
21. E. Grosso, M. Tistarelli, "Active/Dynamic stereo vision," IEEE Trans. On Pattern Analysis and Machine Intelligence, Vol. 7, pp. 868-879, 1995.
22. R. G. Hutchins and LTJG J. P. C. Roque, "Filtering and Control of an Autonomous Underwater Vehicle for both Target Intercept and Docking," Proceedings of the 4th IEEE International Conference on Control Applications, pp. 1162-1163, 1995.
23. Jang, J., Sun, C. and E. Mizutani, Neuro-Fuzzy and Soft Computing, Prentice-Hall, 1997.
24. Joung, I. S., Cho, H. S. "Self-localization for Mobile robot navigation using an Active Omni-directional Range Sensor," Journal of the Korean Society of Precision Engineering, Vol. 16, No. 1, 1999.